

**Statistical significance of tropical cyclone forward speed on storm surge generation: retrospective analysis of best track and tidal data in Japan**

Md. Rezuanul Islam\* and Hiroshi Takagi

*School of Environment and Society, Tokyo Institute of Technology, Tokyo, Japan*

\*corresponding author: [islam.m.ac@m.titech.ac.jp](mailto:islam.m.ac@m.titech.ac.jp)

# **Statistical significance of tropical cyclone forward speed on storm surge generation: retrospective analysis of best track and tidal data in Japan**

## **Abstract**

In this study, 42 years of tidal records and landfall TC best tracks in Japan were used to demonstrate that TC pre-landfall forward speed is significantly correlated with maximum storm surge height. Coastal morphology was the determining factor for the correlation between storm surge and TC forward speed. Fast-moving TCs tended to amplify the storm surge along open coastlines (Pearson correlation coefficient,  $R = 0.62$ ), but reduce it in semi-enclosed bays ( $R = -0.52$ ). The negative correlation contrasts with the general perception that the coincidence of TC wind speed and forward speed vectors generates a larger storm surge. The influence of coastal morphology was most prominent for TCs with a central pressure lower than 956 hPa. Tropical cyclone (TC) operational forecasts are continuously improving; however, there is still scope to improve the precision of storm surge predictions. These findings could contribute to the improvement of storm surge forecasting and provide emergency management personnel with more precise early warnings of dangerous storm surges.

Keywords: tropical cyclone, storm surge, forward speed, coastal morphology, Japan

## **Introduction**

In recent decades, the reliability of storm surge modelling has improved considerably, however, recent major tropical cyclones (TCs) have highlighted the need for increasingly reliable real time storm surge prediction. In the past 15 years, Hurricane Katrina (2005), Cyclone Sidr (2007), Cyclone Nargis (2008), and Typhoon Haiyan (2013) have each caused more than 1,000 fatalities, many of which were the direct result of the storm surge (Esteban, Takagi, and Shibayama 2015). The Saffir–Simpson hurricane wind scale (SSHWS) (previously known as Saffir–Simpson hurricane scale or SSHS) has been used for nearly five decades by meteorologists, weather forecasters, and decision makers to classify TC surface wind speeds and it has become the standard index for forecasting both wind intensity and storm surge. While the use of the SSHWS has several advantages, this simple classification method is limited in

terms of providing a precise estimation of storm surge height. One of the major shortcomings of the wind speed-based scale is an inability to account for other crucial factors that directly influence storm surge generation (Needham and Keim 2011).

Physics-based TC surge modelling has revealed that wind speed is not the only, storm parameter that can markedly influence surge extent. Landfall location, direction of approach, and size have also been demonstrated to have an impact. For example, Sebastian et al. (2014) found that storm surge behaviour in a relatively small water basin such as Galveston Bay in the USA (approximately 1554 km<sup>2</sup>) is highly sensitive to the local wind direction associated with hurricane landfall location. This finding supported the conclusion of Weisberg and Zheng (2006) who revealed that the worst storm surge event would occur in Tampa Bay (USA) when a hurricane makes landfall to the north of the bay, as this would result in the occurrence of maximum winds at the mouth (i.e. the south) of the bay. Irish, Resio, and Ratcliff (2008) evaluated the relationship between hurricane size and maximum storm surge for different bottom slopes. Their results demonstrated that storm surges tend to increase with hurricane size and that this relationship becomes increasingly pronounced for milder sloping coastal bathymetry. Consequently, a range of different scales and indices for storm surge prediction have been investigated considering the importance of TC parameters. For example, Powell and Reinhold (2007) proposed a surge damage potential scale based on the integrated kinetic energy of the TC wind field. While Kantha (2008) suggested a non-dimensional relationship for estimating surge potential based on TC intensity and size. However, both these approaches were questioned by Jordan and Clayson (2008) and Irish and Resio (2010), who claimed that these indices could not replace the SSHWS because neither considered the forward speed of the TC, approach angle, or regional bathymetry pertaining to the surge response. Irish and Resio (2010) developed a hydrodynamics-based storm surge scale that took the TC intensity, size, and slope of the shelf into account. Although this scale has an extensive theoretical and

mathematical background, the assumption that neglects the influence of TC forward speed—made during the derivation of the scale—has been questioned (Kantha 2010).

The importance of TC forward speed for a reliable storm surge/wind-wave prediction has been recognised in numerous studies. For example, Mei, Pasquero, and Primeau (2012) used 40 years of global TC best track data to demonstrate that TC mean translation speed was positively correlated with TC intensity, and faster storms had a greater likelihood of attaining a higher intensity. Using TC data archives from 1948 to 2017, Hall and Kossin (2019) suggested that the amount of local TC related rainfall was inversely proportional to the translation speed of the TC. Takagi et al. (2017), Takagi, Xiong, and Furukawa (2018), and Takagi, Xiong, and Fan (2019) investigated Typhoon Haiyan (2013) in the Philippines and, Typhoon Hato (2017) and Typhoon Mangkhut (2018) in Macau, and demonstrated that local authorities had limited preparation time to respond to these fast-moving typhoons. A numerical study of wind waves in Typhoon Vera (1959) suggested that the maximum wave height tended to increase with the typhoon speed up to 45 km/h, while the extent of the high wave area was large in the case of a slow-moving typhoon (Uji 1975). Typhoon Faxai (2019) generated high waves that led to extensive overtopping damage in a part of Yokohama Port. This typhoon was strong and moved slowly over Tokyo Bay. The main cause of the high waves generated by Faxai was not the swell from the open ocean (i.e., the Pacific Ocean), but the wind waves that developed rapidly within the bay (Takagi et al. 2020). Jelesnianski (1972) performed numerical experiments considering a standard hurricane and found that a fast TC ( $> 48.2$  km/h) tended to intensify the storm surge on hypothetical shelves. A numerical simulation of the Louisiana–Texas shelf during Hurricane Rita (2005) demonstrated that a decrease in TC forward speed resulted in reduced peak surge heights while increasing the inland floodwater discharge volume (Rego and Li 2009). This tendency was also reported by Wei et al. 2019, who used TC Xavier (2013) as a reference storm; they demonstrated that slower storm propagation speed resulted

in a small surge but enhanced the potential of the largest flood area along North Sea coasts. Thomas et al. (2019) also suggested that when a slow TC adopted a shore-parallel course, more seawater tended to accumulate in bays, causing extensive flooding along the coastline from Florida to North Carolina. However, Peng, Xie, and Pietrafesa (2004) used numerical models to investigate the storm surge over an estuary in the same region and found that both the surge height and inundation areas decreased as hurricane forward speed increased. Another study investigated the Charleston Harbour in South Carolina and demonstrated that storm surge height was influenced by TC forward speed and the distance of the track from the harbour (Peng, Xie, and Pietrafesa 2006). Sahoo and Bhaskaran (2017) performed numerical experiments on the coast of Odisha in India and found that in an outer region of the radius of maximum wind ( $R_{\max}$ ), the storm surge height tended to increase with an increase in transition speed; the inverse relationship appeared to be true within the  $R_{\max}$ . Although these numerical sensitivity studies investigated storm surges under different landfall forward speed conditions, they considered hypothetical TCs that ran either parallel or perpendicular to the coastline over small idealised coasts. However, despite historical TC records, less attention has been paid to the impact of TC forward speed on coastal storm surges. To the best of our knowledge, the interaction between landfall or pre-landfall TC forward speed and storm surge has not been investigated using long-term tidal observations over a large area (i.e., for a country or globally).

In this study, the relationship between landfall or pre-landfall TC forward speed and the resultant storm surge heights in Japan were examined for a total of 62 landfall TCs by analysing tidal records from 1978–2019 at 17 tide stations (Figure 1). Japan was chosen due to its geographical uniqueness of the various coastlines, which allows for the investigation of TCs impacting both open coasts and semi-enclosed bays. Furthermore, the Japan Meteorological Agency (JMA) provides an easily accessible and extensive long-term dataset pertaining to TC best track and tide data. For the first time, we attempt to determine whether there is a significant

relationship between TC forward speed and coastal geometry, considering the difference either semi-enclosed bays or open coasts.

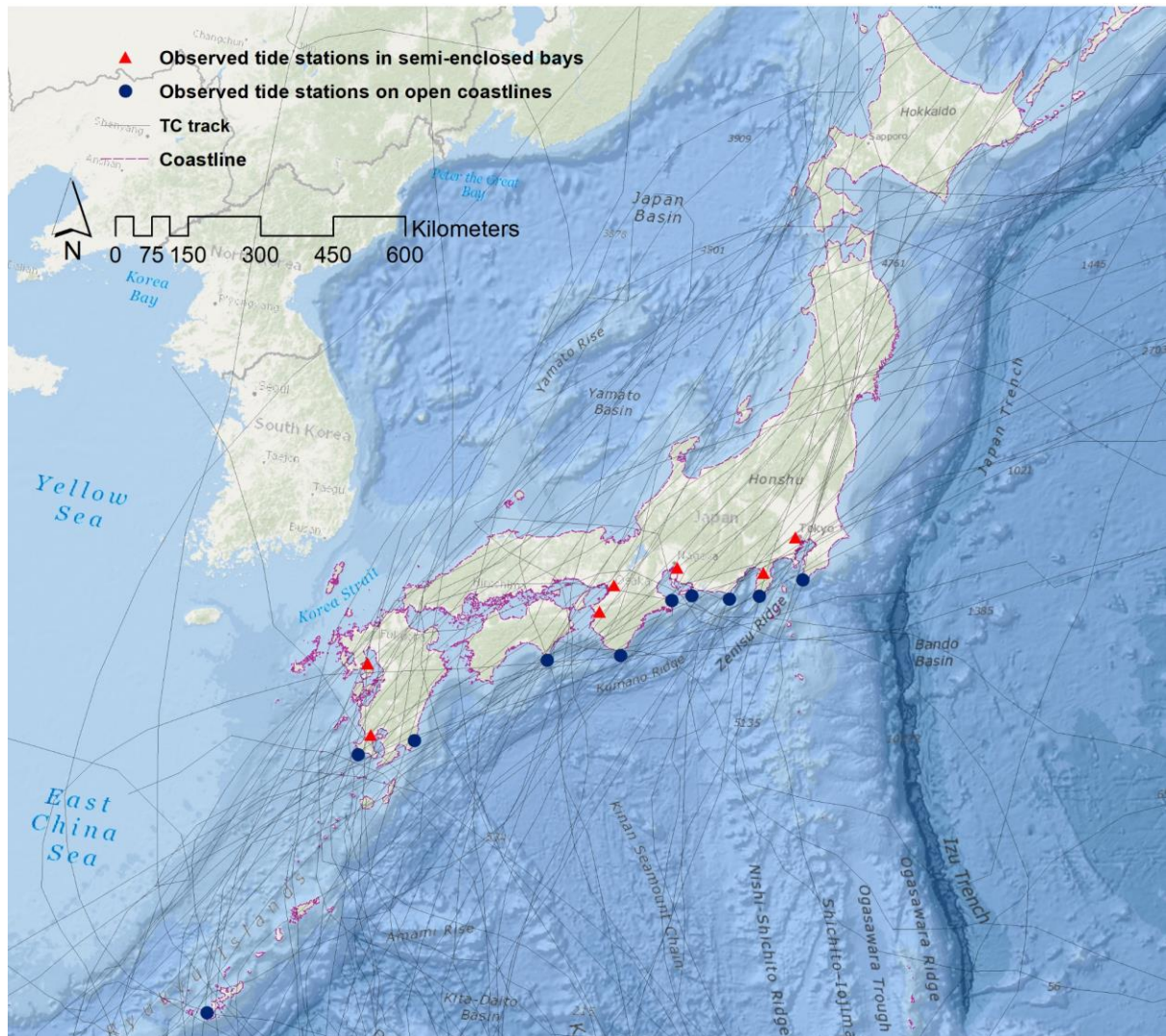


Figure 1. Best track for historical tropical cyclones (TCs) (JMA 2020a) making landfall during 1978–2019 over the four major Japanese islands (Honshu, Shikoku, Kyushu, and Okinawa) based on data from the Japan Meteorological Agency.

## **Materials and Methods**

Best track data from 1978–2019 were retrieved from the JMA archives, including data pertaining to TCs that originated in the North Pacific Ocean and made landfall in Japan (JMA 2020a). Six-hourly data were available over the duration of each TC. To ensure robustness of

the data, best-track data from 1978-onward was used as official operations of Japan's first geostationary meteorological satellite began in 1978 (JMA 2020b). The estimation of TC forward speeds in the pre-satellite era (i.e., before 1978) may not be sufficiently accurate because of uncertainties in tracking, limitations in measurement, and changes in measurement practices (Chan 2019; Moon, Kim, and Chan 2019). In this study, only TCs that made landfall over the major Japanese islands with a maximum sustained wind speed of over 33 m/s (64 kt), equivalent to Category 1 in the SSHWS, were considered. Based on this criterion, 71 TCs were selected for analysis. However, reliable storm surge information was not available for nine TCs, because the astronomical tide table reference elevation for tide stations closest to the tracks was unavailable. Hence, these nine storms were excluded, leaving a total of 62 analysable TC landfall events. The TCs were further divided into two subcategories based on landfall location: open coastlines and bay areas. Of the 62 TCs, 19 made landfall directly over open coastlines, while 18 directly hit bay areas. The remaining 25 TCs made landfall between open coastlines and bay areas and impacted both regions. Additionally, 13 (12) TCs impacted more than 1 tide station located on the open coastlines (bay areas). As a result, there were 62 and 55 available cases for open coasts and bay areas, respectively. Although the sample size ( $n$ ) used in this study was not very large, the period from 1978 to 2019 is the longest time period covered by the JMA best track that ensures the same data quality and consistency.

TC forward speed was estimated by linearly interpolating the speeds at two positions along each TC track. To avoid the influence of the land on transition speed, TC parameters after landfall over the main islands were not analysed in this study.

The TC size information depicted in Figure 5 was retrieved from the JMA best track archives. Both the radius of maximum wind ( $R_{\max}$ ) and the radius of the wind with a speed of 26 m/s (50 kt;  $R_{50}$ ) are the two spatial parameters that directly represent the TC size (Takagi and Wu 2016). As  $R_{\max}$  is not included in the JMA best track dataset (JMA, 2020a), this study

used  $R_{50}$ —which is defined as the maximum radial extent (in nautical miles) of the wind reaching a speed of 50 kt. For cases in which  $R_{50}$  information was unavailable during TC landfall time,  $R_{50}$  was obtained via linear interpolation of the available data at two neighbouring positions (immediately before and after landfall).

Figure 1 shows the 17 JMA-operated tide stations (JMA 2020c) that were used to estimate the peak storm surge for each TC. Although other tide stations were operational, data collection was restricted to stations satisfying the following criteria: (a) located on open coastline or in a bay; (b) located closest to historical TC tracks; (c) JMA predicted astronomical tide data were available (JMA 2020d); (d) elevation of the observation reference plane and the astronomical tide table reference plane were available; and (e) no data were missing when a TC traversed the station. Based on these criteria, ten stations (Naha, Makurazaki, Aburatsu, Murotomisaki, Kushimoto, Toba, Akabane, Omaezaki, Irouzaki, and Mera) were selected as representative observatories for storm surges on open coastlines and seven stations (Oura, Kagoshima, Osaka, Wakayama, Nagoya, Uchiura, and Harumi) were selected as representative observatories for storm surges in semi-enclosed bays (regions surrounded by two land areas that form a concave-shaped coastline). Figure 2 provides details of the selected tide stations. Sea surface anomalies were assumed to be the storm surge magnitude, and they were estimated by deducting the predicted astronomical tide from the observed storm tide.

To investigate the role of TC forward speed on storm surge potential, the statistical correlation between the observed TC forward speed and storm surge height was tested. A dataset comprising the normalized peak storm surge and forward speed at landfall, six, and 12 hours prior to landfall, was used for the analysis. Several factors, including wind intensity, central pressure, forward speed, and TC size contribute to the surge that a TC produces. As the maximum wind speed of a TC is directly proportional to the square root of the central pressure deficit ( $\Delta p$ ) (Holland 1980), the storm surge was scaled by dividing the peak surge by  $\Delta p$  (=

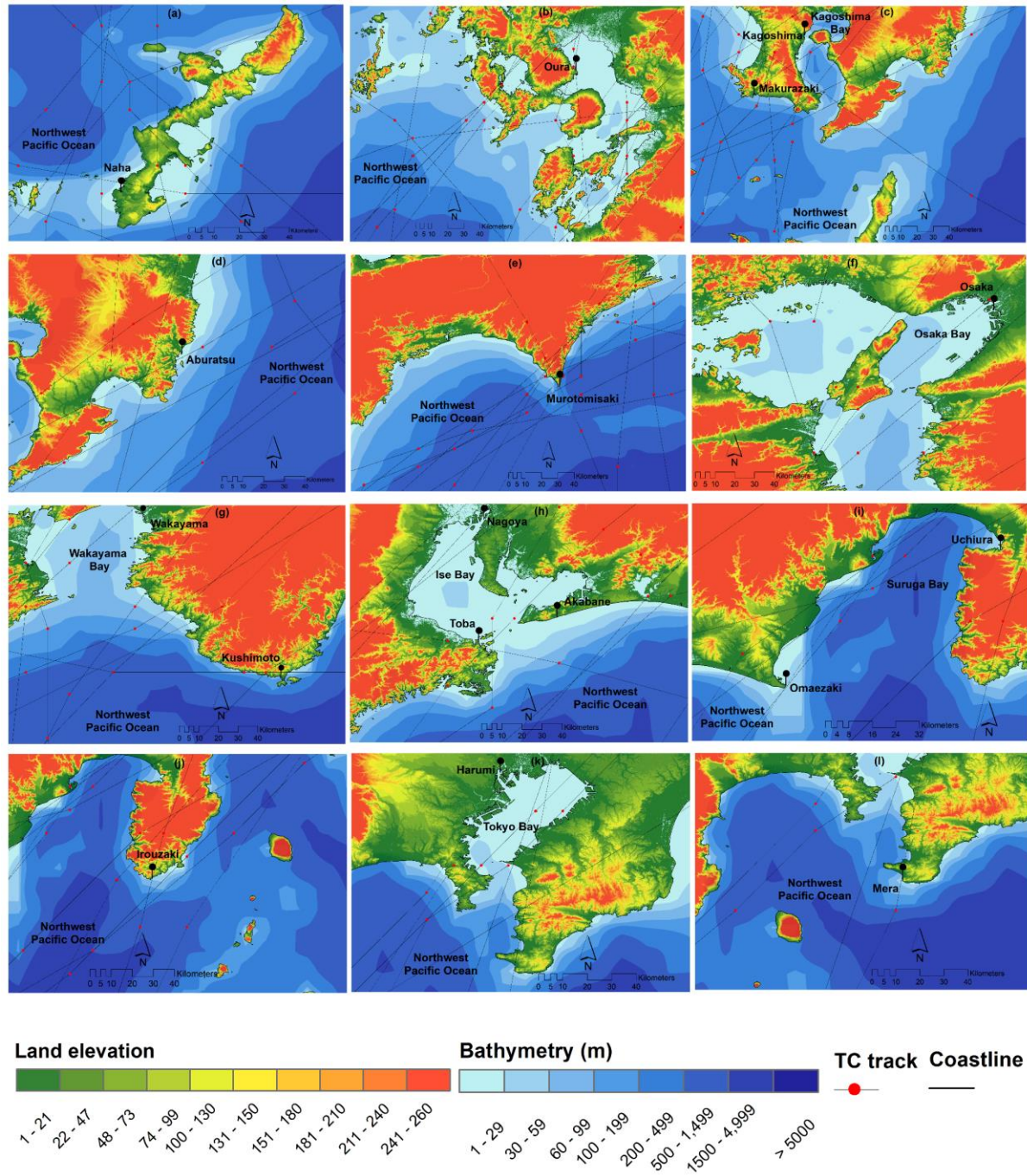


Figure 2. Location map of observed tide stations (a) Naha, Okinawa island; (b) Oura, Kyushu island; (c) Makurazaki and Kagoshima, Kyushu island; (d) Aburatsu, Kyushu island; (e) Murotomisaki, Shikoku island; (f) Osaka, Honshu island; (g) Wakayama and Kushimoto, Honshu island; (h) Toba, Nagoya, and Akabane, Honshu island; (i) Omaezaki and Uchiura, Honshu island; (j) Irouzaki, Honshu island; (k) Harumi, Honshu island; (l) Mera, Honshu island; (JODC, 2000; JAXA, 2015; GSI Japan, 2016; JMA, 2020a).

mean sea level pressure, 1013 hPa – pressure at the centre of the TC) to eliminate the effect of TC intensity prior to analysis. Subsequently, statistical analyses were performed separately for TCs that made landfall along open coastlines and in bays. Correlation analyses were conducted for the groups of different TC intensities, which were classified based on (a) intensity at landfall time and (b) subsequent levelling of the sample size among the intensity categories. Three categories were defined in this study: (1) TCs with  $\Delta p > 57$  hPa ( $n = 24$ , open coasts;  $n = 20$ , bays), (2) TCs with  $\Delta p = 48\text{--}57$  hPa ( $n = 25$ , open coasts;  $n = 15$ , bays), and (3) TCs with  $\Delta p < 48$  ( $n = 13$ , open coasts;  $n = 20$ , bays). The historically strongest TCs—such as Mireille (1991), Nabi (2005), Goni (2015), Jebi (2018), and Hagibis (2019)—fall in the first group while moderate and weaker TCs belong to the second and third group, respectively.

The Pearson correlation coefficient ( $R$ ), was used to measure the strength of the linear association between the observed TCs' forward speed and normalized peak storm surge height. The  $p$ -values of the correlation statistics were calculated based on the two-tailed 95% confidence level test.

## **Results**

Figure 3 (a) and (b) show the correlation between the average 12 h pre-landfall forward speed (calculated by averaging the observed speeds at 0, 6, and 12 h prior to landfall;  $FS_{avg}$ ) and the scaled maximum storm surge height. Fast moving TCs tended to amplify the surge height along open coastlines ( $R = 0.62$ ;  $p < .01$ ), whereas reduce the height in semi-enclosed bays ( $R = -0.52$ ;  $p < .01$ ). Similarly, we performed correlation analysis between the TC landfall forward speed ( $FS_L$ ) and corresponding scaled maximum storm surge height to determine whether another variation of the TC forward speed would have a better correlation as compared to that of the  $FS_{avg}$ . The  $R$  values of the linear regression for open coastlines and semi-enclosed bays were 0.65 ( $p < .01$ ) and -0.47 ( $p < .01$ ), respectively, similar to those of the  $FS_{avg}$ . While the

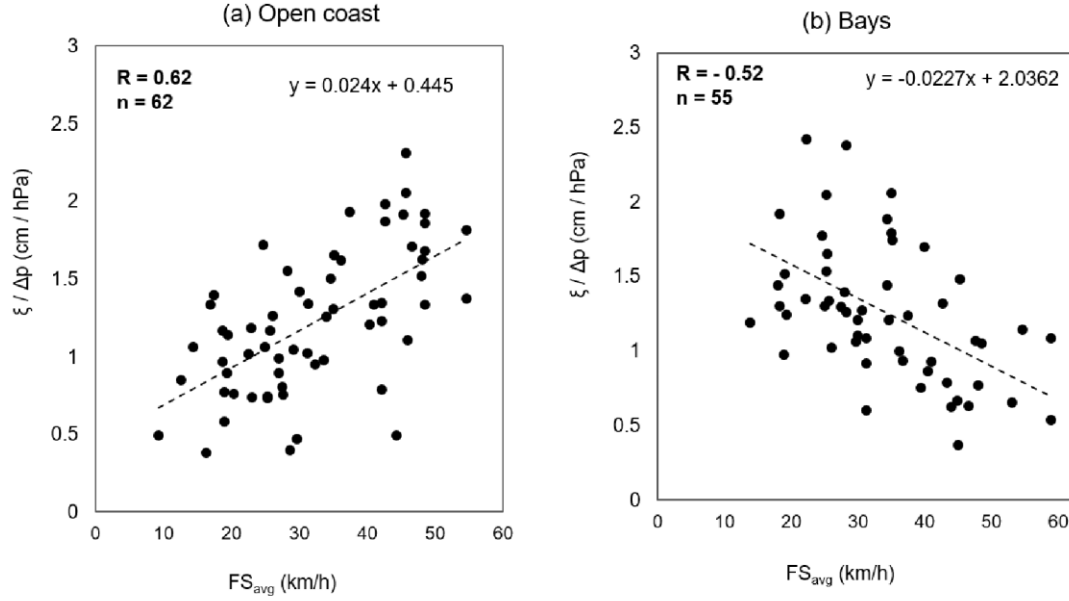


Figure 3. Observed TC surges ( $\xi$ ) normalised by the central pressure deficit ( $\Delta p$ ) versus the 12 h averaged forward speed before landfall ( $FS_{avg}$ ) for (a) open coastlines and (b) bays. Dashed lines show the correlation gradient of the respective normalised surge ( $\xi$ ) and  $FS_{avg}$ .

surge variance for  $FS_L$  was slightly higher (3.81%) for open coastlines, it was lower (4.95%) for semi-enclosed bays. We tested the association between  $FS_L$  and  $FS_{avg}$ , which resulted in a strong correlation statistic of 0.93. We conclude that for this sample of landfall TCs,  $FS_{avg}$  is as good an indicator of the maximum storm surge, like  $FS_L$ .

Correlations corresponding to the 6 h averaged pre-landfall forward speed, 6 h and 12 h prior to landfall forward speed, were calculated to explore whether any other definition of forward speed would provide better correlations compared to  $FS_{avg}$ . These results (not provided in this study) did not vary markedly from the statistics presented in Figure 3. Additionally, correlations corresponding to the database and excluding the three highest observed storm surges, caused by Typhoon Melor (2009) and Typhoon Trami (2018) in open coastlines and Typhoon Fitow (2007), Typhoon Roke (2011), and Typhoon Hagibis (2019) in semi-enclosed bays, were made to ensure that the outliers were not skewing the Pearson statistics shown in Figure 3. The resulting Pearson correlations were 0.58 and -0.48 for open coastlines and semi-

enclosed bays, respectively. Therefore, although the correlations changed due to the removed outliers,  $FS_{avg}$  were still statistically correlated with the scaled peak storm surge heights. Hence, the average 12 h pre-landfall forward speed can provide a reasonably accurate estimation of the maximum storm surge for a TC making landfall. Furthermore, pre-landfall average forward speed is beneficial for storm surge prediction as it contributes to precise early warning and better emergency management before typhoon landfall.

The dataset in Figure 3 was reanalysed, as shown in Figure 4, to demonstrate that the relationship between TC forward speed and storm surge was most prominent for stronger TCs with a central pressure deficit greater than 57 hPa (central pressure < 956 hPa;  $R$  of 0.80 and -0.60 for open coastlines and semi-enclosed bays, respectively). For open coastlines, the correlation gradient increased with a deficit in pressure, resulting in an improvement of up to

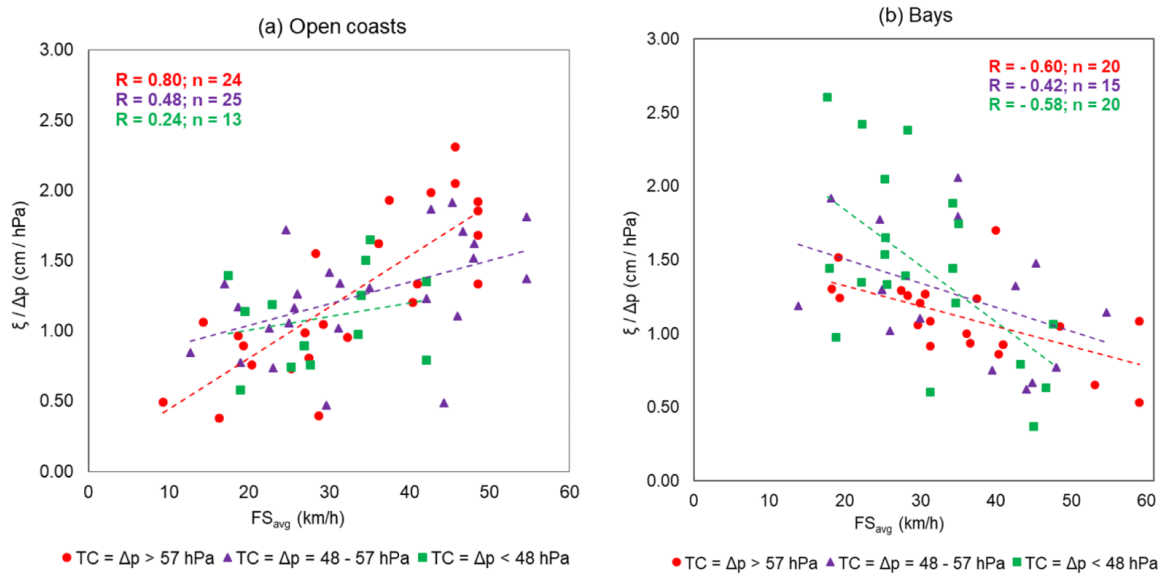


Figure 4. Normalised storm surges ( $\xi/\Delta p$ ) versus the 12 h averaged TC forward speed ( $FS_{avg}$ ), grouped by the central pressure deficit ( $\Delta p$ ) for (a) open coastlines and (b) semi-enclosed bays. Dashed lines show the correlation gradient of the normalised surge and forward speed for each group.

58% in the estimation of storm surge variance (Figure 4 (a)). Conversely, the change in the correlation gradient was relatively small for semi-enclosed bays (Figure 4 (b)). However, the influence of slow moving (i.e.,  $FS_{avg} < 40$  km/h), intense storms (i.e.,  $\Delta p > 57$  hPa) on the generation of a larger surge in semi-enclosed bays was apparent. Figure 4 also demonstrates that less intense TCs ( $\Delta p \leq 57$  hPa) tended to generate smaller storm surges along open coastlines and semi-enclosed bays, independent of whether they were slow or fast moving.

The influence of another important parameter, TC size, was investigated to determine if a better correlation with storm surge height compared to the TC forward speed was present. Results indicated no significant relationship between TC size and coastal geometry (Figure 5). Although large TCs tended to amplify the surge height along open coastlines ( $R = 0.35$ ;  $p < .01$ ), there was no significant influence on the storm surge height in semi-enclosed bays ( $R = -0.03$ ;  $p = 0.82$ ).

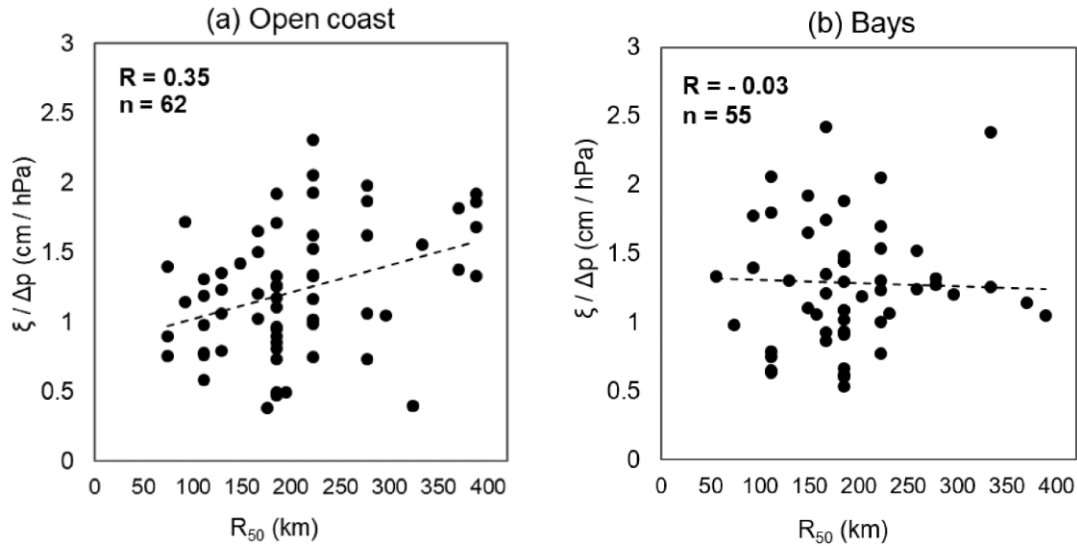


Figure 5. Observed TC surges ( $\xi$ ) normalised by the central pressure deficit ( $\Delta p$ ) versus landfall size ( $R_{50}$ ) for (a) open coastlines and (b) bays. Dashed lines show the correlation gradient of the respective normalised surges ( $\xi$ ) and  $R_{50}$ .

## **Discussion**

The TC pre-landfall average forward speed is significantly correlated with the observed maximum storm surge height. Open coastlines and semi-enclosed bays exhibited opposite correlation tendencies. Faster ( $FS_{avg} > 40$  km/h) and more intense (central pressure  $< 956$  hPa) TCs are likely to produce larger storm surges along open coastlines; this is consistent with the idealized TC studies (e.g. Jelesnianski 1972; Rego and Li 2009; Thomas et al. 2019). For example, TCs with a  $FS_{avg} > 34$  km/h (average  $FS_{avg}$  of TCs that made landfall in Japan = 34 km/h) generated an average surge height of 0.84 m, while TCs with  $FS_{avg} \leq 34$  km/h produced an average height of 0.52 m. The variances in the many recorded significant storm surge events could also be partially explained by the differences in the TC forward speed. For instance, TC Trami (2018) (Figure 6) which was the largest storm surge event recorded at the Murotomisaki Station in the past 42 years (JMA 2020c), generated a maximum storm surge height of 1.15 m (JMA 2020c). This TC was characterised as a fast-moving ( $FS_{avg} = 43$  km/h) and strong TC ( $\Delta p = 58$  hPa; maximum sustained wind speed = 40 m/s). Although the average intensity 18 h prior to landfall was the same at the time of landfall, the  $FS_{avg}$  was comparatively faster than the historically observed average TC transitional speed of 30 km/h in the respective region (Shikoku island). Typhoon Etau (2003), a relatively slow ( $FS_{avg} = 29$  km/h) TC, took a similar path and had a similar intensity ( $\Delta p = 63$  hPa; maximum sustained wind speed = 40 m/s) as Typhoon Trami and made landfall at Murotomisaki (Figure 6) (JMA 2020a). However, the observed maximum storm surge height was 57.4% (0.66 m) (JMA 2020c) lower than that of TC Trami. This difference may have been caused by the slight difference in the paths of the storms. Etau followed a western path, while Trami followed an eastern path to the tidal station (Murotomisaki) and, thus, changed its wind direction; which tended to lower the storm surge. It is also plausible that a fast-moving TC would energise a shelf wave and cause an increased storm surge because the TC translation speed tends to coincide with the long wave propagation

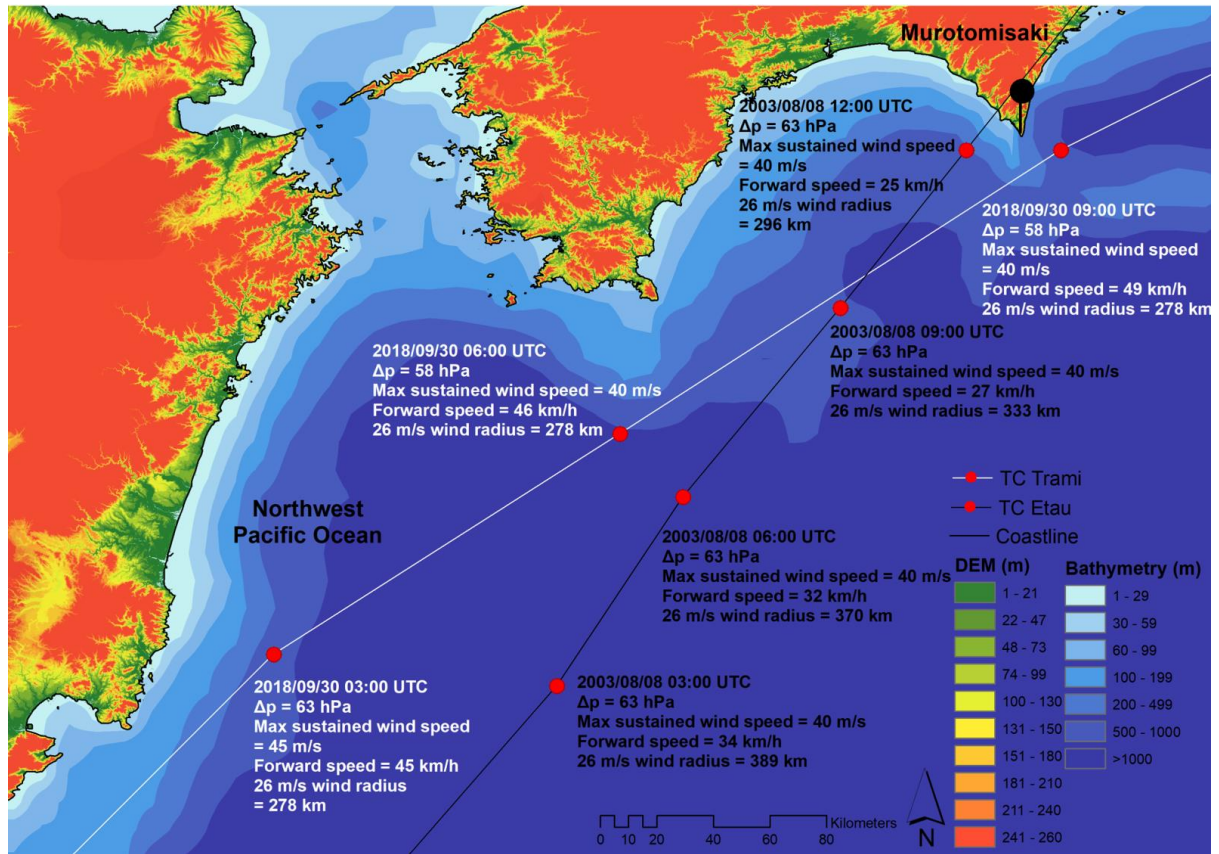


Figure 6. TCs Trami and Etai as it approached Murotomisaki, Shikoku island (JODC, 2000; JAXA, 2015; GSI Japan, 2016; JMA, 2020a).

speed (Thomas et al. 2019). This mechanism could be partially explained by the linear theory of Proudman (1952), which showed that storm surges could be amplified when the TC translation speed was similar to the propagation speed of the long wave ( $\sqrt{gh}$ ). For TC Trami, the  $FS_{avg}$  was 43 km/h and corresponded to a long wave for depths of 14 m. Although the isobaths varied in their distances offshore (Figure 6), they were within the location at which the increased peak storm surge was observed. However, not all fast moving TCs generate a higher peak surge because other factors may drive surge variability.

In contrast, a slower TC can generate a higher surge in a semi-enclosed bay. This agrees with the previous idealized TC studies (Peng 2004; Weisberg and Zheng 2006), but is contrary to results of Rego and Li (2009) and Wei et al. (2019). These numerical sensitivity analyses

are based solely on an idealized coast that may not capture all the details of coastal topography. Additionally, the analyses were carried out for a small geographic location (limited variations in coastlines). However, storm surges are highly dependent on local features, coastline shapes, and the width and slope of the ocean bottom. Therefore, it is possible that—depending on the set-up condition and limitations of the numerical model—similar studies can result in different conclusions.

The storm surge history of the semi-enclosed bays in Japan provides evidence for an inverse relationship between surge magnitude and TC forward speed. For example, TCs with a  $FS_{avg} \leq 34$  km/h generated an average surge height of 0.74 m, while TCs with a  $FS_{avg} > 34$  km/h produced an average height of 0.56 m in semi-enclosed bays. A comparison between TC Danas (2001) and TC Higos (2002) provided a clear contrast. Both these TCs took a similar path and made landfall at the Miura peninsula adjacent to Tokyo Bay (Figure 7). TC Higos was a faster ( $FS_{avg} = 59$  km/h) and stronger TC (960 hPa), which generated a peak surge level of 0.63 m in Harumi (0.90 m in Mera). Danas was a slower ( $FS_{avg} = 18$  km/h) and weaker TC (965 hPa), but it generated a peak surge of 1.12 m (0.74 m in Mera). This led to substantial damage in the coastal areas of Tokyo.

In semi-enclosed bays, the effective cross-shore shallow area over which TC winds act is larger. As a result, the contribution of wind stress tends to be more pronounced in the bay than the open coastlines due to a shallower depth (e.g. Mastenbroek, Burgers, and Janssen 1993). Also, the time scale for mass redistribution (to generate a sea surface slope) within the shallow and geometrically complex estuaries is in the order of hours and somewhat longer than along the open coasts (Weisberg and Zheng 2006). Thereby, with cross-shore wind stress components, a slower TC has more time to interact with the seawater and pushes more into shallow areas of a bay. Consequently, surge height begins to fully develop (or mature), causing a large sea-level gradient between the upper and lower bay. This phenomenon is contrary to

the general perception that the coincidence of wind and forward speed vectors generate a larger storm surge.

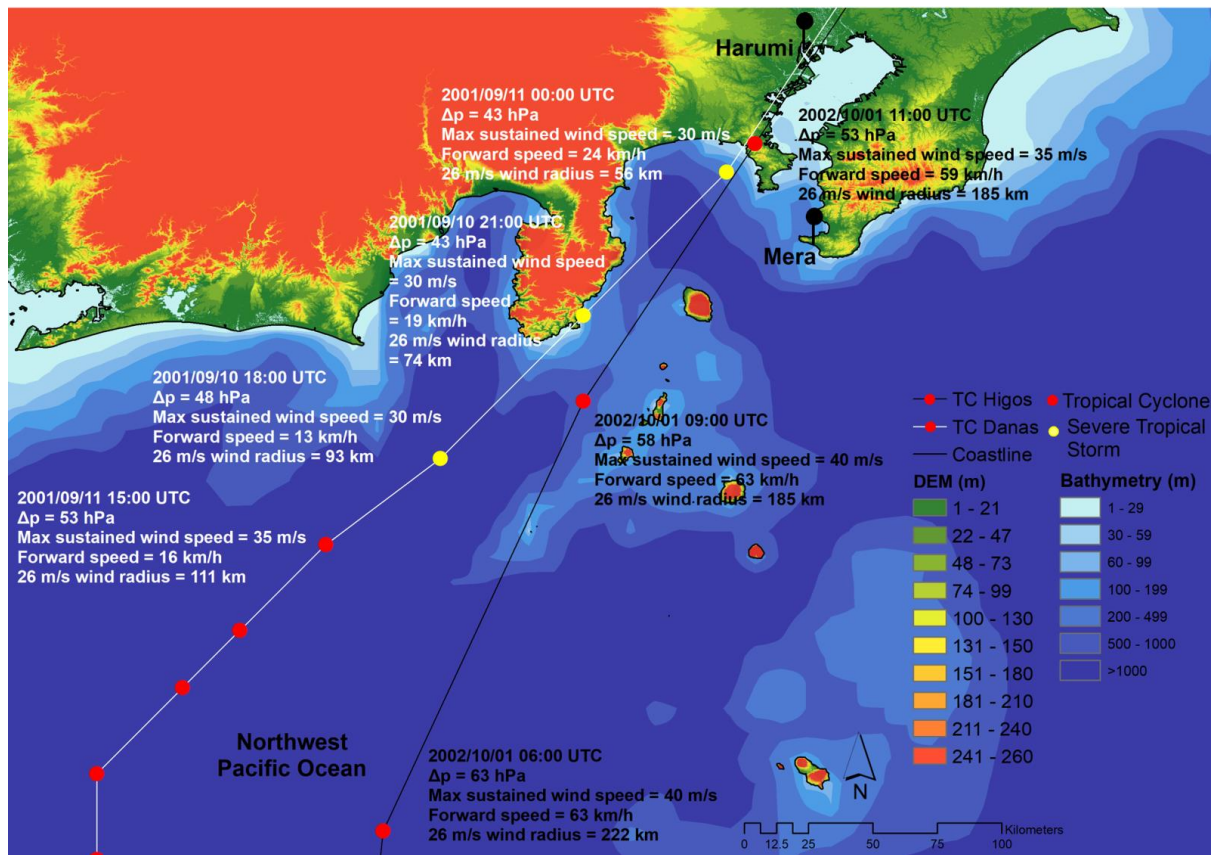


Figure 7. TCs Danas and Higos as it approached Harumi, Honshu island (JODC, 2000; JAXA, 2015; GSI Japan, 2016; JMA, 2020a).

## Conclusion

For decades, scientists have focused on numerical sensitivity analysis to explain the relative importance of TC forward speed. However, these numerical analyses have not been sufficiently compared with long term observations. The analysis presented herein demonstrates variances in the maximum storm surge height with TC forward speed and coastal geometry. Our findings may be beneficial in two main areas. Firstly, considering TC transitional speed and coastal geometry (open coastline or bays) - meteorologists and oceanographers could provide more comprehensive surge forecasts, and emergency management personnel could use pre-landfall average forward speed for more precise early warning. Secondly, coastal areas at risk of storm

surge with no access to advanced surge models could use these empirical findings along with other TC intensity related information to estimate the maximum surge heights and improve evacuation plans. However, varying TC transitional speed influences not only the storm surge height but also the flood volume, which was not addressed in this study. Further research in this area should also examine the influence of changes in geographic location (i.e., for another country or globally), as this can influence the characteristics of storm surge distribution.

### **Acknowledgments**

The first author is thankful to the Ministry of Education, Culture, Sports, Science, and Technology (MEXT) of Japan for the provided scholarship to conduct research in the field of disaster risk reduction. This research was funded by a grant awarded to the Tokyo Institute of Technology (Japan Society for the Promotion of Science, 16KK0121 and 19K04964). Best track TC data for 1979–2018 (<https://www.jma.go.jp/jma/jma-eng/jma-center/rsmc-hp-pub/trackarchives.html>), and observed (<http://www.data.jma.go.jp/kaiyou/db/tide/genbo/index.php>) and predicted (<http://www.data.jma.go.jp/kaiyou/db/tide/suisan/index.php>) tide data were provided by the Japan Meteorological Agency.

### **Disclosure statement**

No potential conflict of interest was reported by the author(s).

### **Funding**

This work was supported by a grant awarded to the Tokyo Institute of Technology (Japan Society for the Promotion of Science) [grant number 16KK0121, 19K04964]

## References

- Chan, K. T. F. 2019. “Are global tropical cyclones moving slower in a warming climate?” *Environmental Research Letters* 14 (104015). [doi.org/10.1088/1748-9326/ab4031](https://doi.org/10.1088/1748-9326/ab4031)
- Esteban, M., H. Takagi, and T. Shibayama. 2015. “Lessons from the last 10 years of coastal disasters.” In *Handbook of Coastal Disaster Mitigation for Engineers and Planners*, edited by M. Esteban, H. Takagi, T. Shibayama, xxv-xxx. Oxford: Butterworth Heinemann.
- Geospatial Information Authority of Japan. 2016. GSI Japan Global map site (accessed July 4, 2019). [https://www.gsi.go.jp/kankyochiri/gm\\_japan\\_e.html](https://www.gsi.go.jp/kankyochiri/gm_japan_e.html).
- Hall, T. M., and J. P. Kossin. 2019. “Hurricane stalling along the North American coast and implications for rainfall.” *Npj Climate and Atmospheric Science* 2 (17). [doi.org/10.1038/s41612-019-0074-8](https://doi.org/10.1038/s41612-019-0074-8)
- Holland, G. J. 1980. “An Analytic Model of the Wind and Pressure Profiles in Hurricanes.” *Monthly Weather Review* 108 (8): 1212–1218. [doi:10.1175/1520-0493\(1980\)108<1212:AAMOTW>2.0.CO;2](https://doi.org/10.1175/1520-0493(1980)108<1212:AAMOTW>2.0.CO;2).
- Irish, J. L., D. T. Resio, and J. J. Ratcliff. 2008. “The Influence of Storm Size on Hurricane Surge.” *Journal of Physical Oceanography* 38 (9): 2003–2013. [doi: 10.1175/2008JPO3727.1](https://doi.org/10.1175/2008JPO3727.1).
- Irish, J. L., and D. T. Resio. 2010. “A Hydrodynamics-Based Surge Scale for Hurricanes.” *Ocean Engineering* 37: 69–81. [doi: 10.1016/j.oceaneng.2009.07.012](https://doi.org/10.1016/j.oceaneng.2009.07.012).
- Japan Oceanographic Data Center. 2000. 500 m Gridded Bathymetric Feature Data around Japan. (accessed July 4, 2019). [https://jdoss1.jodc.go.jp/vpage/depth500\\_file.html](https://jdoss1.jodc.go.jp/vpage/depth500_file.html).
- Japan Aerospace Exploration Agency. 2015. 30 m World Elevation Data Site. (accessed July 4, 2019). <https://www.eorc.jaxa.jp/ALOS/en/aw3d30/data/index.htm>.
- Japan Meteorological Agency. 2020a. Typhoon Best Track Data Site. (accessed Jan 10, 2020). <https://www.jma.go.jp/jma/jma-eng/jma-center/rsmc-hp-pub-eg/trackarchives.html>.
- Japan Meteorological Agency. 2020b. History of Japan’s Geostationary Meteorological Satellite site. (accessed Jan 10, 2020). <https://www.jma-net.go.jp/sat/himawari/enkaku.html>.]
- Japan Meteorological Agency. 2020c. Tidal Observation Data Site. (accessed January 10, 2020). <http://www.data.jma.go.jp/kaiyou/db/tide/genbo/index.php>.

- Japan Meteorological Agency. 2020d. Astronomic Tide Prediction Data Site. (accessed January 10, 2020). <http://www.data.jma.go.jp/kaiyou/db/tide/suisan/index.php>.
- Jelesnianski, C. P. 1972. SPLASH (Special Program to List Amplitudes of Surges from Hurricanes): 1. Landfall storms. In *NOAA Technical Memorandum NWS TDL-46*. Silver Spring, MD: NOAA.
- Jordan, M. R. and C. A. Clayson. 2008. "Evaluation of usefulness of a new set of hurricane classification indices." *Monthly Weather Review* 136 (12): 5234–5238. doi: [10.1175/2008MWR2449.1](https://doi.org/10.1175/2008MWR2449.1).
- Kantha, L. 2008. "Comments: Tropical Cyclone Destructive Potential by Integrated Kinetic Energy." *Bulletin of the American Meteorological Society* 88 (2): 219–221.
- Kantha, L. 2010. "Discussion of "A hydrodynamics-based surge scale for hurricanes." *Ocean Engineering* 37 (11-12): 1081–1084. doi:[10.1016/j.oceaneng.2010.04.003](https://doi.org/10.1016/j.oceaneng.2010.04.003)
- Mastenbroek, C., G. Burgers, and P. A. E. M. Janssen. 1993. "The Dynamical Coupling of a Wave Model and a Storm Surge Model through the Atmospheric Boundary Layer." *Journal of Physical Oceanography* 23 (8): 1856–1866. doi: [10.1175/15200485\(1993\)023<1856:TDCOAW>2.0.CO;2](https://doi.org/10.1175/15200485(1993)023<1856:TDCOAW>2.0.CO;2).
- Mei, W., C. Pasquero, and F. Primeau. 2012. "The Effect of Translation Speed upon the Intensity of Tropical Cyclones over the Tropical Ocean." *Geophysical Research Letters* 39: L07801. doi: [10.1029/2011GL050765](https://doi.org/10.1029/2011GL050765).
- Moon, I.-J., S.-G. Kim, & J.C.L. Chan. 2019. "Climate change and tropical cyclone trend." *Nature* 570: E3-E5. doi:[10.1038/s41586-019-1222-3](https://doi.org/10.1038/s41586-019-1222-3)
- Needham, H. F., and B. D. Keim. 2011. "Storm Surge: Physical Processes and an Impact Scale." In *Recent Hurricane Research—Climate, Dynamics, and Societal Impacts*, edited by A. Lupo, 386–394. London: IntechOpen.
- Peng, M., L. Xie, and L. J. Pietrafesa. 2004. "A Numerical Study of Storm Surge and Inundation in the Croatan-Albemarle-Pamlico Estuary System." *Estuarine Coastal Shelf Science* 59 (1): 121–137. doi: [10.1016/j.ecss.2003.07.010](https://doi.org/10.1016/j.ecss.2003.07.010).
- Peng, M., L. Xie, and L. J. Pietrafesa. 2006. "A Numerical Study on Hurricane-Induced Storm Surge and Inundation in Charleston Harbor, South Carolina." *Journal of Geophysical Research* 111: C08017. doi: [10.1029/2004JC002755](https://doi.org/10.1029/2004JC002755).
- Powell, M. D., and T. A. Reinhold. 2007. "Tropical Cyclone Destructive Potential by Integrated Kinetic Energy." *Bulletin of the American Meteorological Society* 88 (4): 513–526. doi: [10.1175/BAMS-88-4-513](https://doi.org/10.1175/BAMS-88-4-513).

- Proudman, J. 1953. *Dynamical Oceanography*. New York: Wiley.
- Rego, J. L., and C. Li. 2009. "On the Importance of the Forward Speed of Hurricanes in Storm Surge Forecasting: A Numerical Study." *Geophysical Research Letters* 36: L07609. [doi: 10.1029/2008GL036953](https://doi.org/10.1029/2008GL036953).
- Sahoo, B., and P. K. Bhaskaran. 2018. "A comprehensive data set for tropical cyclone storm surge-induced inundation for the east coast of India." *International Journal of Climatology*, 38: 403–419. [doi.org/10.1002/joc.5184](https://doi.org/10.1002/joc.5184)
- Sebastian, A. G., J. M. Proft, J. C. Dietrich, W. Du, P. B. Bedient, and C. N. Dawson. 2014. "Characterizing Hurricane Storm Surge Behavior in Galveston Bay Using the SWAN + ADCIRC Model." *Coastal Engineering* 88: 171–181. [doi: 10.1016/j.coastaleng.2014.03.002](https://doi.org/10.1016/j.coastaleng.2014.03.002).
- Takagi, H., and W. Wu. 2016. "Maximum wind radius estimated by the 50 kt radius: improvement of storm surge forecasting over the western North Pacific." *Natural Hazards and Earth System Sciences* 16: 705–717. [doi: 10.5194/nhess-16-705-2016](https://doi.org/10.5194/nhess-16-705-2016)
- Takagi, H., M. Esteban, T. Shibayama, T. Mikami, R. Matsumaru, M. De Leon, N. D. Thao, T. Oyama, and R. Nakamura. 2017. "Track Analysis, Simulation, and Field Survey of the 2013 Typhoon Haiyan Storm Surge." *Journal of Flood Risk Management* 10 (1): 42–52. [doi: 10.1111/jfr3.12136](https://doi.org/10.1111/jfr3.12136).
- Takagi, H., Y. Xiong, and F. Furukawa. 2018. "Track Analysis and Storm Surge Investigation of 2017 Typhoon Hato: Were the Warning Signals Issued in Macau and Hong Kong Timed Appropriately?" *Georisk: Assessment and Management of Risk for Engineered Systems and Geohazards* 12: 297–307. [doi: 10.1080/17499518.2018.1465573](https://doi.org/10.1080/17499518.2018.1465573).
- Takagi, H., Y. Xiong, and J. Fan. 2019. "Public Perception of Typhoon Signals and Response in Macau: Did Disaster Response Improve between the 2017 Hato and 2018 Mangkhut." *Georisk: Assessment and Management of Risk for Engineered Systems and Geohazards* [doi: 10.1080/17499518.2019.1676453](https://doi.org/10.1080/17499518.2019.1676453).
- Takagi, H., M. R. Islam, L. T. Anh, A. Takahashi, T. Sugiu, and F. Furukawa. 2020. "Investigation of high wave damage caused by 2019 Typhoon Faxai in Kanto region and wave hindcast in Tokyo Bay." *Journal of Japan Society of Civil Engineers B3 (Ocean Engineering)* 76 (1). [doi: 10.2208/jscejoe.76.1\\_12](https://doi.org/10.2208/jscejoe.76.1_12)
- Thomas, A., J. C. Dietrich, T. G. Asher, M. Bell, B. O. Blanton, J. H. Copeland, A. T. Cox, C. N. Dawson, J. G. Fleming, and R. A. Luettich. 2019. "Influence of Storm Timing

- and Forward Speed on Tides and Storm Surge during Hurricane Matthew.” *Ocean Modelling* 137: 1-19. [doi: 10.1016/j.ocemod.2019.03.004](https://doi.org/10.1016/j.ocemod.2019.03.004).
- Uji, T. 1975. “Numerical Estimation of the Sea Wave in a Typhoon Area.” *Meteorology and Geophysics* 28 (4): 199–217. [doi.org/10.2467/mripapers1950.26.4\\_199](https://doi.org/10.2467/mripapers1950.26.4_199)
- Weisberg, R. H., and L. Zheng. 2006. “Hurricane Storm Surge Simulations for Tampa Bay.” *Estuaries and Coasts* 29 (6): 899–913. [doi: 10.1007/BF02798649](https://doi.org/10.1007/BF02798649).
- Wei, X., J. M. Brown, J. Williams, P. D. Thorne, M. E. Williams and L. O. Amoudry. 2019. “Impact of storm propagation speed on coastal flood hazard induced by offshore storms in the North Sea.” *Ocean Modelling* 143. [doi: 10.1016/j.ocemod.2019.101472](https://doi.org/10.1016/j.ocemod.2019.101472)